Electronic Supplementary Information (ESI)

Post-synthetic metal-ion metathesis in a single-crystal-to-single-crystal process: improving the gas adsorption and separation capacity of an indium-based metal-organic framework

Shuang Liu,[a, b] Bing Liu,[b] Shuo Yao,*[a, b] and Yunling Liu*[b]

[a] *College of Chemistry and Chemical engineering, Ocean University of China, Qingdao 266100, P. R. China*

[b] *State Key Laboratory of Inorganic Synthesis and Preparative Chemistry, College of Chemistry, Jilin University, Changchun 130012, P. R. China. E-mail: yunling@jlu.edu.cn; Fax: +86-431-85168624; Tel: +86-431-85168614*

S1. Supporting Figures

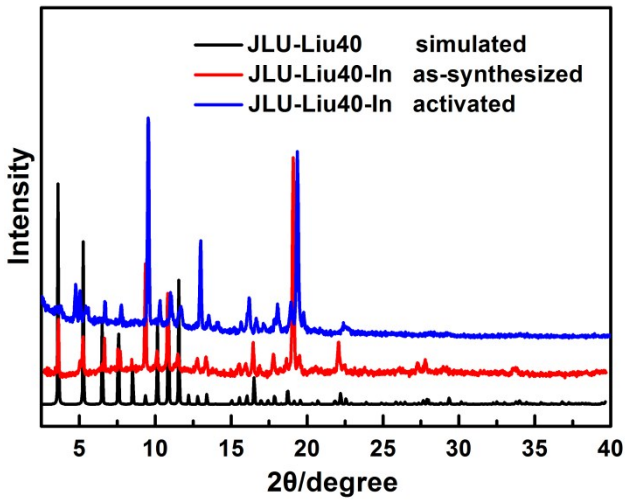

Fig. S1. PXRD patterns of as-synthesized and activated **JLU-Liu40-In** corresponding to the simulated **JLU-Liu40**.

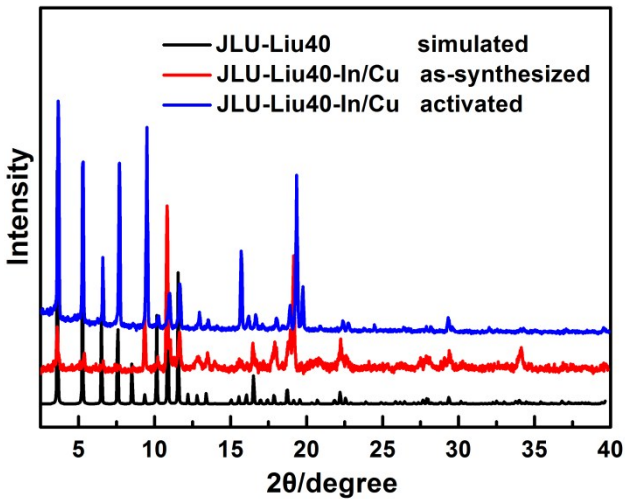

Fig. S2. PXRD patterns of as-synthesized and activated **JLU-Liu40-In/Cu** corresponding to the simulated **JLU-Liu40**.

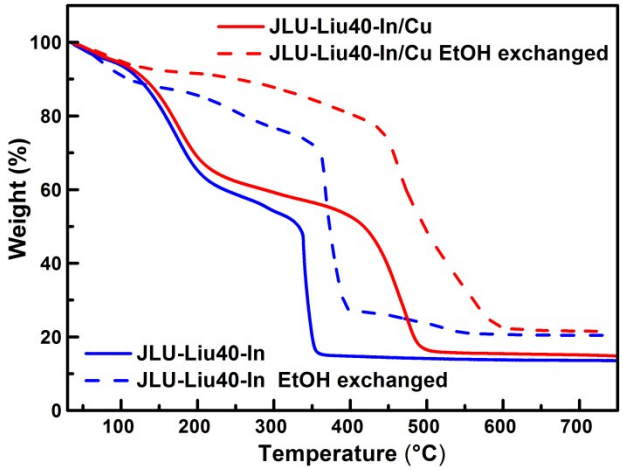

Fig. S3 Thermogravimetric analysis curves of **JLU-Liu40-In** and **JLU-Liu40-In/Cu** for the as-synthesized and EtOH exchanged compounds.

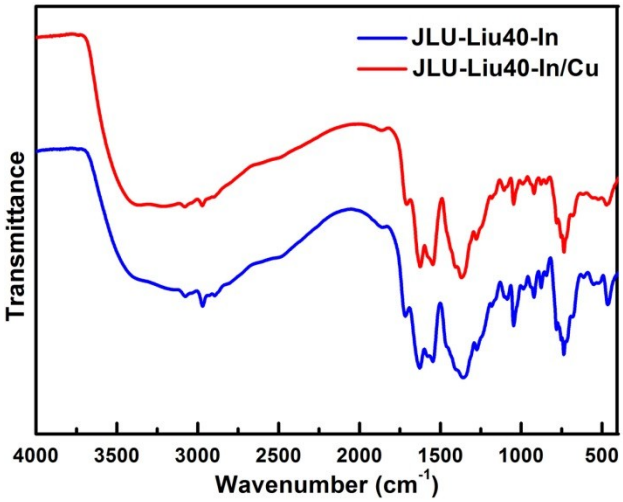

Fig. S4 Infrared spectra of **JLU-Liu40-In** and **JLU-Liu40-In/Cu** (KBr, cm^{-1}).

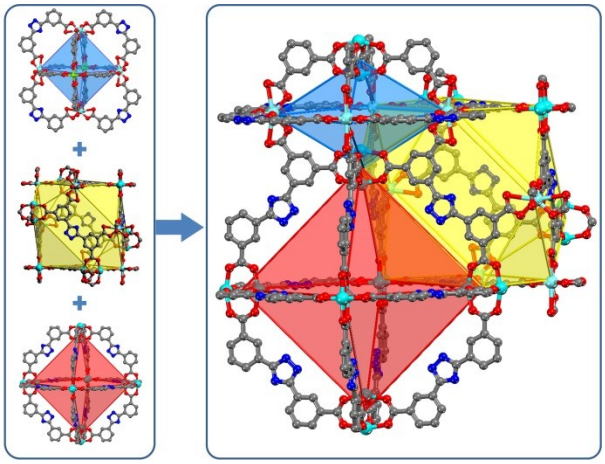

Fig. S5 View of the three different cages and the arrangement in **JLU-Liu40-In** as representative.

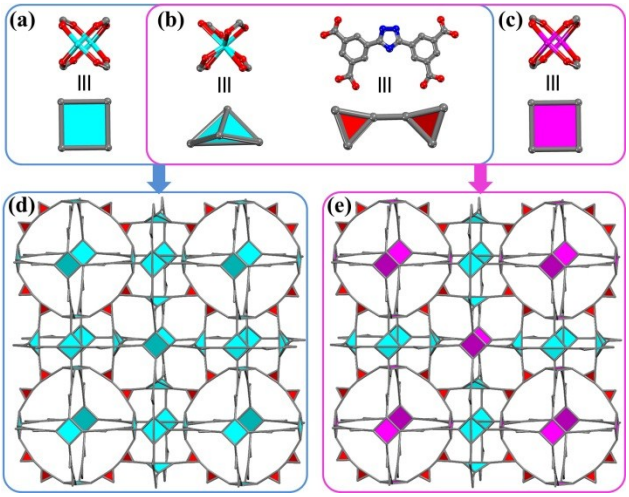

Fig. S6 (a) In-paddlewheel simplified as 4-connected square; (b) mononuclear In and organic $TADIPA^{4-}$ linker simplified as tetrahedron and a pair of 3-connected triangle, respectively; (c) Cu-paddlewheel simplified as 4-connected square; (d) polyhedron view of **JLU-Liu40-In**; (e) polyhedron view of **JLU-Liu40-In/Cu**.

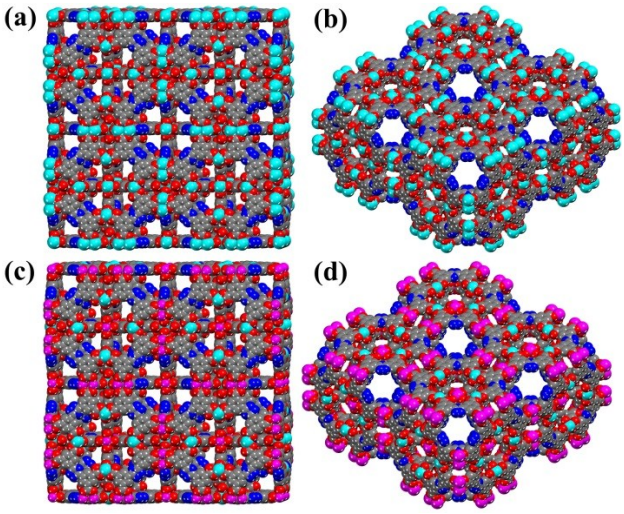

Fig. S7 Space-filling model of **JLU-Liu40-In** along the [001], [010], [100] (a) and [111] (b) directions; Space-filling model of **JLU-Liu40-In/Cu** along the [001], [010], [100] (c) and [111] (d) directions. (Color scheme: carbon, gray; oxygen, red; nitrogen, blue; indium, cyan; copper, pink.)

S2. Supporting Tables

Table S1 Gas adsorption information of heterometallic cluster-based In-MOFs.

Compounds	Hetero-metal	Surface areas[a]		Gas uptakes					Ref.
		BET	Langmuir	H_2[b]	CO_2[c]	CH_4[c]	C_2H_6[c]	C_3H_8[c]	
JLU-Liu40-In/Cu	In/Cu	1763	2381	230/ 138	123/ 60	26/ 14	199/ 113	231/ 205	this work
InOF-2-Li^+	In/Li	1494	1652	217.7/ 137.5	125.2/ 60.8	25.5/ 15.5	N.A.	N.A.	1
CPM-200-In/Mg	In/Mg	1374	1883	312.9/ N.A.	190.8/ 113.7	41.8/ 25.1	N.A.	N.A.	2
CPM-200-In/Co	In/Co	1040	1446	208.9/ N.A.	136.9/ 77.6	30.0/ 17.9	N.A.	N.A.	2
$[InCu(OH)(CPT)_2]\cdot(NO_3)_2\cdot(DMF)_4$	In/Cu	1032	N.A.	N.A.	N.A. /53.4	N.A./ 13.1	N.A.	N.A.	3
CPM-20	In/Co	1009	1134	195.4/ N.A.	91.2/ 47.7	N.A.	N.A.	N.A.	4
In/Cu-CBDA	In/Cu	990	1169	N.A.	76/ 40	12/ 6	114/ 67	127/ 112	5
CPM-200s-In/Mn	In/Mn	941	1303	197.7/ N.A.	126.5/ 72.7	26.7/ 16.1	N.A.	N.A.	2
$In_3Mg(IMDC)_3(NO_3)_2(H_2O)_6\cdot$solvent	In/Mg	902	1057	130.71/ N.A.	58.36/ ~41	N.A.	N.A.	N.A.	6
CPM-200-In/Ni	In/Ni	877	1216	179.6/ N.A.	100.4/ 61.5	25.9/ 15.7	N.A.	N.A.	2
$[Me_2NH_2][In(L)]$-Li^+	In/Li	820	1024	N.A.	N.A.	N.A.	N.A.	N.A.	7
$[(CH_3)_2NH_2][In_3Ca_2(BTC)_4(DMF)_2(H_2O)_4Cl_2]\cdot$solvent	In/Ca	805	975	162.79/ N.A.	94.33/ 55.59	12.75/ ~56	N.A.	N.A.	8
$[In_3O(L)1.5(H_2O)_2Cl]\cdot$n(solv)	In/Pd	795	851	N.A.	92.3/ N.A.	N.A.	N.A.	N.A.	9
$In_3Mn(IMDC)_3(NO_3)_2(H_2O)_6\cdot$solvent	In/Mn	790	921	128.52/ N.A.	51.78/ ~32	N.A.	N.A.	N.A.	6
In/Tb-CBDA	In/Tb	782	866	N.A.	64/ 35	13.5/ 8	80/ 50	82/ 61	10
$[(CH_3)_2NH_2][In_3Sr_2(BTC)_4(DMF)_2(H_2O)_4Cl_2]\cdot$solvent	In/Sr	654	831	146.78/ N.A.	76.71/ ~48	16.94/ ~47	N.A.	N.A.	8
$[(CH_3)_2NH_2][In_3Ba_2(BTC)_4(DMF)_2(H_2O)_4Cl_2]\cdot$solvent	In/Ba	570	699	103.89/ N.A.	68.65/ 41.52	7.22/ ~42	N.A.	N.A.	8
InOF-7	In/Cu	526	637	~60/ N.A.	~45 N.A.	N.A.	N.A.	N.A.	11
$In_3Co(IMDC)_3(NO_3)_2($	In/Co	483	576	104.44/	47.74/	N.A.	N.A.	N.A.	6

$H_2O)_6$·solvent				N.A.	~29				
$In_3Zn(IMDC)_3(NO_3)_2(H_2O)_6$·solvent	In/Zn	378	449	78.08/ N.A.	45.49/ ~29	N.A.	N.A.	N.A.	6
BUT-52	In/Cu	358	522	N.A.	57.9/ 26.5	13.2/ 7.7	71.6/ 40.7	N.A.	12
CPM-19-Nd	In/Nd	272	370	147.8/ N.A.	38.4/ N.A.	N.A.	N.A.	N.A.	4
$Co_5In(BTC)_4[B_2O_4(OH)]_2$	In/Cu/B	248.0	N.A.	N.A.	N.A.	N.A.	N.A.	N.A.	13
InOF-6	In/Cu	89.8	113.2	~26/ N.A.	N.A.	N.A.	N.A.	N.A.	11
InOF-8	In/Cu	N.A.	N.A.	95.2/ 66.6	66.2/ N.A.	16.6/ N.A.	N.A.	N.A.	14

[a]At 77 K and 1.0 bar, $m^2\ g^{-1}$.

[b]At 77 K/87 K and 1.0 bar, $cm^3\ g^{-1}$.

[c]At 273 K/298 K and 1.0 bar, $cm^3\ g^{-1}$.

N.A. Not Available. The article does not list the data.

References:

1. J. Qian, F. Jiang, D. Yuan, X. Li, L. Zhang, K. Su and M. Hong, Increase in pore size and gas uptake capacity in indium-organic framework materials, *J. Mater. Chem. A*, 2013, **1**, 9075-9082.
2. Q. G. Zhai, X. Bu, C. Mao, X. Zhao and P. Feng, Systematic and dramatic tuning on gas sorption performance in heterometallic metal-organic frameworks, *J. Am. Chem. Soc.*, 2016, **138**, 2524-2527.
3. F. Gao, Y. Li, Y. Ye, L. Zhao, L. Chen and H. Lv, A heterometallic approach for enhancing the net robustness of metal-organic framework, *Inorg. Chem. Commun.*, 2017, **80**, 72-74.
4. S. T. Zheng, T. Wu, C. Chou, A. Fuhr, P. Feng and X. Bu, Development of composite inorganic building blocks for MOFs, *J. Am. Chem. Soc.*, 2012, **134**, 4517-4520.
5. D. Wang, Y. Zhang, J. Gao, G. Ge and C. Li, A Polyhedron-based heterometallic MOF constructed by HSAB theory and SBB strategy: synthesis, structure, and adsorption properties, *Cryst. Growth Des.*, 2019, **19**, 4571-4578.
6. C.-C. Deng, X.-X. Li, Y.-J. Qi, X. Ma, S.-T. Zheng and Q.-X. Zeng, Construction of four indium-based heterometallic metal-organic frameworks containing intersecting indium-organic helical chains and different divalent-metal-ion linkers, *Eur. J. Inorg. Chem.*, 2017, **2017**, 4919-4924.
7. S. Yang, X. Lin, A. J. Blake, K. M. Thomas, P. Hubberstey, N. R. Champness and M. Schroder, Enhancement of H_2 adsorption in Li^+-exchanged co-ordination framework materials, *Chem. Commun.*, 2008, **46** , 6108-6110
8. Y.-J. Qi, D. Zhao, X.-X. Li, X. Ma, W.-X. Zheng and S.-T. Zheng, Indium-based heterometal-organic frameworks with different nanoscale cages: syntheses, structures, and gas adsorption properties, *Cryst.Growth Des.*, 2017, **17**, 1159-1165.
9. I. Bratsos, C. Tampaxis, I. Spanopoulos, N. Demitri, G. Charalambopoulou, D. Vourloumis, T. A. Steriotis and P. N. Trikalitis, Heterometallic In(III)-Pd(II) porous metal-organic framework

with square-octahedron topology displaying high CO_2 uptake andselectivity toward CH_4 and N_2, *Inorg. Chem.*, 2018, **57**, 7244-7251.
10. D. Wang, Z. Liu, L. Xu, C. Li, D. Zhao, G. Ge, Z. Wang and J. Lin, A heterometallic metal-organic framework based on multi-nuclear clusters exhibiting high stability and selective gas adsorption, *Dalton Trans.*, 2018, **48**, 278-284.
11. J. Qian, F. Jiang, K. Su, J. Pan, L. Liang, F. Mao and M. Hong, Constructing crystalline heterometallic indium-organic frameworks by the bifunctional method, *Cryst. Growth Des.*, 2015, **15**, 1440-1445.
12. Y. Han, H. Zheng, K. Liu, H. Wang, H. Huang, L. H. Xie, L. Wang and J. R. Li, In-situ ligand formation-driven preparation of a heterometallic metal-organic framework for highly selective separation of light hydrocarbons and efficient mercury adsorption, *ACS Appl. Mater. Interfaces*, 2016, **8**, 23331-23337.
13. S. Y. Li and Z. H. Liu, $Co_5In(BTC)_4[B_2O_4(OH)]_2$: the first MOF material constructed by borate polyanions and carboxylate mixed ligands, *Dalton Trans.*, 2016, **45**, 66-69.
14. J. Qian, F. Jiang, K. Su, J. Pan, Z. Xue, L. Liang, P. P. Bag and M. Hong, Heterometallic cluster-based indium-organic frameworks, *Chem. Commun.*, 2014, **50**, 15224-15227.

Table S2 Gas adsorption and separation information of **JLU-Liu40-In** and **JLU-Liu40-In/Cu**.

Compounds	Surface areas[a]		Gas uptakes					Selectivity		
	BET	Langmuir	H_2[b]	CO_2[c]	CH_4[c]	C_2H_6[c]	C_3H_8[c]	CO_2/ CH_4[d]	C_2H_6/ CH_4[e]	C_3H_8/ CH_4[e]
JLU-Liu40-In	1083	1464	149/ 91	89/ 45	19/ 10	125/ 73	143/ 127	1.7/ 1.1	1.3	2.8
JLU-Liu40-In/Cu	1763	2381	230/ 138	123/ 60	26/ 14	199/ 113	231/ 205	4.6/ 3.8	32	177
Increment /%	62.8	62.6	54.4/ 51.6	38.2/ 33.3	36.8/ 40.0	59.2/ 54.8	61.5/ 61.4	170.6/ 245.5	2361.5	6221.4

[a]At 77 K and 1.0 bar, $m^2\ g^{-1}$. [b]At 77 K/87 K and 1.0 bar, $cm^3\ g^{-1}$. [c]At 273 K/298 K and 1.0 bar, $cm^3\ g^{-1}$. [d]0.5:0.5/0.05:0.95 Mixture. [e]0.5:0.5 Mixture.

S3. Calculation procedures of selectivity from IAST

The measured experimental data is excess loadings (q^{ex}) of the pure components CO_2, CH_4, C_2H_6 and C_3H_8 for **JLU-Liu40-In** and **JLU-Liu40-In/Cu**, which should be converted to absolute loadings (q) firstly.

$$q = q^{ex} + \frac{pV_{pore}}{ZRT}$$

Here Z is the compressibility factor. The Peng-Robinson equation was used to estimate the value of compressibility factor to obtain the absolute loading, while the measure pore volume 0.53 and 0.86 $cm^3\ g^{-1}$ for **JLU-Liu40-In** and **JLU-Liu40-In/Cu** is also necessary.

The dual-site Langmuir-Freundlich equation is used for fitting the isotherm data at 298K.

$$q = q_{m_1} \times \frac{b_1 \times p^{1/n_1}}{1 + b_1 \times p^{1/n_1}} + q_{m_2} \times \frac{b_2 \times p^{1/n_2}}{1 + b_2 \times p^{1/n_2}}$$

Here p is the pressure of the bulk gas at equilibrium with the adsorbed phase (kPa), q is the adsorbed amount per mass of adsorbent (mol kg^{-1}), q_{m1} and q_{m2} are the saturation capacities of sites 1 and 2 (mol kg^{-1}), b_1 and b_2 are the affinity coefficients of sites 1 and 2 (1/kPa), n_1 and n_2 are the deviations from an ideal homogeneous surface.

The selectivity of preferential adsorption of component 1 over component 2 in a mixture containing 1 and 2, perhaps in the presence of other components too, can be formally defined as

$$S = \frac{q_1/q_2}{p_1/p_2}$$

q_1 and q_2 are the absolute component loadings of the adsorbed phase in the mixture. These component loadings are also termed the uptake capacities. We calculate the values of q_1 and q_2 using the Ideal Adsorbed Solution Theory (IAST) of Myers and Prausnitz.

Table S3 The refined parameters for the Dual-site Langmuir-Freundlich equations fit for the pure isotherms of CO_2, CH_4, C_2H_6 and C_3H_8 for **JLU-Liu40-In** at 298 K.

	q_{m1}	b_1	n_1	q_{m2}	b_2	n_2	R^2
CO_2	4.84137	2.27087	3.49754E-5	0.01444	1.8376	0.94683	0.99996
CH_4	1.95396	0.68607	0.00188	0.06017	1.70915	0.99134	0.99993
C_2H_6	8.0737	1.26457	9.84593E-4	0.05067	1.30402	0.90225	0.99998
C_3H_8	4.60302	1.74561	0.10785	0.00224	0.86496	2.34256	0.99998

Table S4. The refined parameters for the Dual-site Langmuir-Freundlich equations fit for the pure isotherms of CO_2, CH_4, C_2H_6 and C_3H_8 for **JLU-Liu40-In/Cu** at 298 K.

	q_{m1}	b_1	n_1	q_{m2}	b_2	n_2	R^2
CO_2	22.71384	0.52804	6.35832E-4	0.03216	1.08827	0.95748	0.99998
CH_4	0.88991	3.06572	1.08738E-6	0.00394	2.68535	1.03352	0.99993
C_2H_6	2.9348	10.86251	0.0317	3.74678E-4	0.93747	1.5018	0.99998
C_3H_8	1.06441	8.34339	1.3564	0.01604	1.25856	1.58706	0.99997

S4. Calculations of the isosteric heats of gas adsorption (Q_{st})

A virial-type expression comprising the temperature-independent parameters a_i and b_j was employed to calculate the enthalpies of adsorption for CH_4, C_2H_6 and C_3H_8 (at 273 and 298 K) on compounds. In each case, the data were fitted using the equation:

$$ln^P = ln^N + {}^1/_T \sum_{i-0}^{m} a_i N^i + \sum_{j-0}^{n} b_j N^j$$

Here, P is the pressure expressed in Torr, N is the amount adsorbed in mmol g^{-1}, T is the temperature in K, a_i and b_j are virial coefficients, m, n represent the number of coefficients required to adequately describe the isotherms (m and n were gradually increased until the contribution of extra added a and b coefficients was deemed to be statistically insignificant towards the overall fit, and the average value of the squared deviations from the experimental values was minimized). The values of the virial coefficients a_0 through a_m were then used to calculate the isosteric heat of adsorption using the following expression.

$$Q_{st} = -R \sum_{i-0}^{m} a_i N^i$$

Q_{st} is the coverage-dependent isosteric heat of adsorption and R is the universal gas constant. The heats of gas sorption for JLU-Liu31 in this manuscript are determined by using the sorption data measured in the pressure range from 0-1 bar (273 and 298 K for gases), which is fitted by the virial-equation very well.

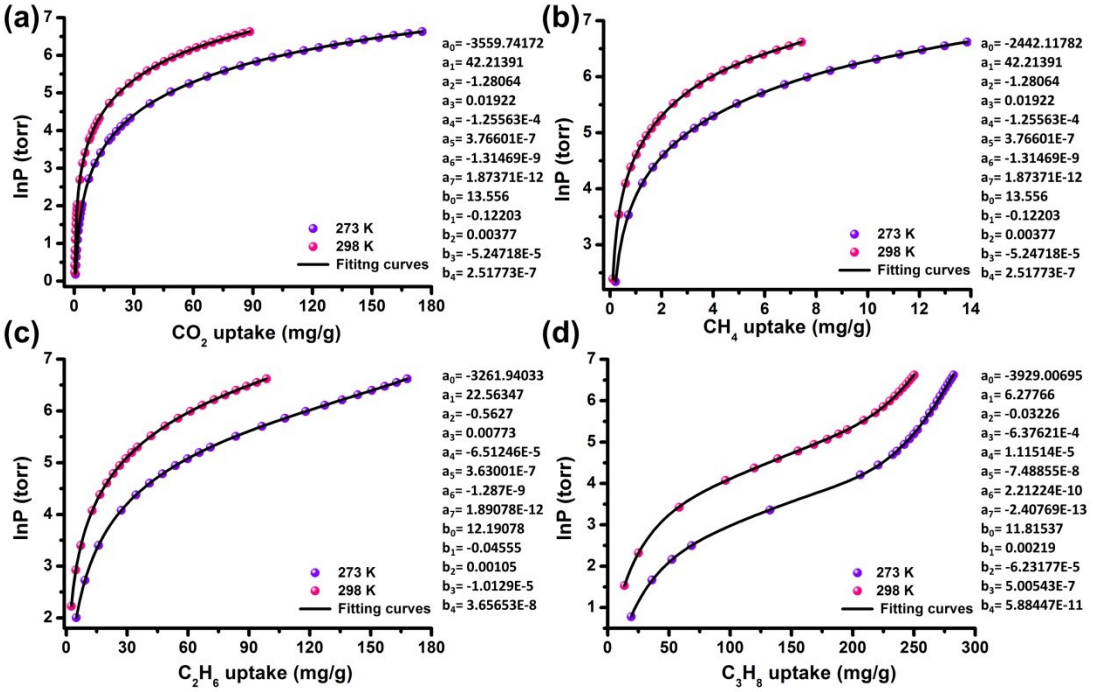

Fig. S8 Nonlinear curves fitting of **JLU-Liu40-In** for CO_2 (a), CH_4 (b), C_2H_6 (c) and C_3H_8 (d) at 273 and 298 K.

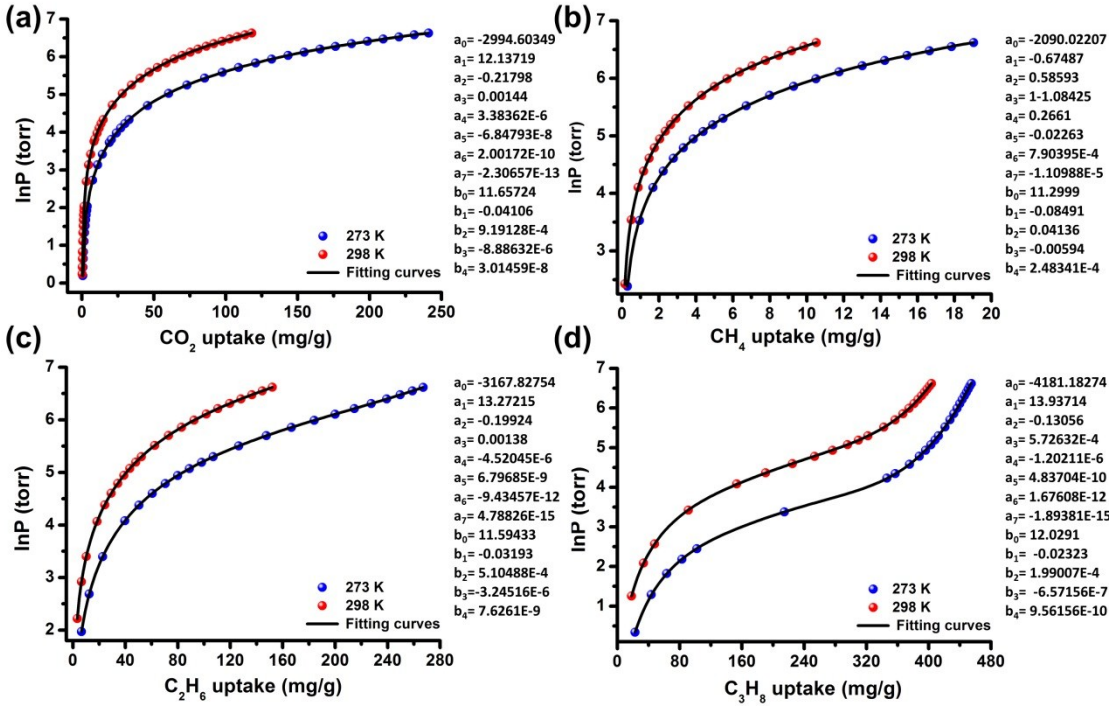

Fig. S9 Nonlinear curves fitting of **JLU-Liu40-In/Cu** for CO_2 (a), CH_4 (b), C_2H_6 (c) and C_3H_8 (d) at 273 and 298 K.